5-1-2020

DEVELOPMENT OF A PROPELLER OPTIMIZATION PROGRAM FOR COMPOUND ROTORCRAFT

Anna Llamas

DEVELOPMENT OF A PROPELLER OPTIMIZATION PROGRAM FOR COMPOUND ROTORCRAFT

by

ANNA LLAMAS

Presented to the Faculty of the Honors College of

The University of Texas at Arlington in Partial Fulfillment

of the Requirements

for the Degree of

HONORS BACHELOR OF SCIENCE IN AEROSPACE ENGINEERING

THE UNIVERSITY OF TEXAS AT ARLINGTON

May 2020

ACKNOWLEDGMENTS

I would like to share of my gratitude to my professor, Dr. Smith, for allowing me the opportunity to complete this additional task for my senior design team's rotorcraft configuration, and for being willing to review my work. I would also like to thank my team, Team #1: FR Aerospace, for the past two semesters of opportunity, creativity and learning.

May 08, 2020

ABSTRACT

DEVELOPMENT OF A PROPELLER OPTIMIZATION PROGRAM FOR COMPOUND ROTORCRAFT

Anna Llamas, B.Sc. Aerospace Engineering

The University of Texas at Arlington, 2020

Faculty Mentor: Dudley Smith

Rotorcraft have been increasingly able to achieve faster flight by considering lighter weight materials, more optimal structural configurations, and auxiliary propulsion units, among several other factors during their design process. The compound coaxial rotorcraft this investigation supported was designed to equip an auxiliary ducted fan to reach and exceed the speed requirements set by the government program it intends to satisfy. A propeller program was developed in conjunction with a ducted fan model to optimize the geometric design decisions and enhance the aircraft configuration.

TABLE OF CONTENTS

Appendix

LIST OF ILLUSTRATIONS

LIST OF TABLES

CHAPTER 1

INTRODUCTION

1.1 FARA

The Future Attack Reconnaissance Aircraft (FARA) program is an initiative by the Unites States government to replace its aging fleet of Vertical/Short Landing or Takeoff (VSTOL) aircraft. A subsidiary to the Future Vertical Lift program, FARA has received submissions from engineering powerhouses such as Boeing, Bell, L3, and Lockheed Martin's Sikorsky. This program aims to produce light and high-speed rotorcraft that may be able to obtain dash speeds in excess of 220 knots true airspeed, with the aircraft's geometry fitting within a forty-foot by forty-eight-foot box. These performance requirements push the envelope of what modern aeronautical technology is capable of producing. Due to these demanding size and airspeed constraints, companies must innovate on past designs in order to produce a competitive product. For example, Sikorsky is fielding its S-97 Raider, a coaxial rotorcraft featuring rigid main rotors with a ducted fan to provide ancillary propulsion. This configuration is known as a "coaxial compound", in reference to the compound thrust and/or lift that the design integrates.

When trying to field high-speed rotorcraft, weight and power savings are incredibly important. The designer must go through meticulous and thorough studies on their components in order to optimize a configuration to obtain the rigorous performance requirements of the FARA program. One such optimization which must be particularly studied is that of the propulsive device on the rotorcraft. Whether the airframe utilizes

ducted fan or a pusher-prop, it is essential the device operates as efficiently as possible. This means the device must be designed to minimize torque, weight, and complexity, while maintaining operational requirements and meetings standards on noise and safety.

1.1.1 Compound Coaxial Helicopter

The FARA program's Request for Proposal (RFP), while classified, may be partially deciphered from open literature. Therefore, it is painfully apparent to the reader that this program seeks to push rotorcraft into unprecedented territory in terms of performance capabilities. As previously mentioned, this indicates innovations must be made to develop a competitive design. In this spirit, a compound coaxial helicopter is selected to be developed by Senior Design Team #1 of UT Arlington's aerospace capstone design project, class of 2020.

The coaxial compound configuration is unique and highly competitive. First, coaxial rotors allow for improved hover performance. Efficiency factors such as the figure of merit are exceptional for this configuration in comparison to more conventional rotorcraft. Also, the rate of climb of a coaxial rotorcraft is able to exceed that of conventional rotorcraft. Secondly, coaxial rotors eliminate the necessity of an anti-torque device. A typical helicopter features a tail rotor, whose sole purpose is to balance the torque induced by the spinning main rotor and allow for yaw control of the aircraft. The tail rotor of the conventional rotorcraft features a high tip speed which creates a very large, undesirable signature. Additionally, the tail rotor is an exceptionally dangerous device on the ground, responsible for loss of life and limb by the ground crew. The coaxial compound eliminates the requirement for such an anti-torque device by utilizing two counter-rotating main rotors. These counter-rotating rotors may be utilized on their own to generate a yaw

force controlled by the aircraft's crew. Finally, the coaxial compound configuration utilizes ancillary lift and propulsion to increase the performance of the aircraft. A rotor alone is not capable of meeting the FARA performance objectives, demonstrated by the results from conventional rotorcraft proposals. Thus, auxiliary lifting and propulsive devices are necessary.

1.1.2 Auxiliary Propulsion

Many options exist for providing thrust offload in forward flight. Ducted fans, turbofans, and even jet engines have been strapped to rotorcraft in the past. However, the FARA RFP indicates that designs are limited to the use of the T-901 turboshaft powerplant.[1] Consequently, engineers are limited to ducted fans and pusher-propellers in their designs.

Pusher-props are merely propellers, as seen in commercial fixed-wing aircraft, positioned in the rear of the rotorcraft. The nose of a rotorcraft is known as "prime real estate," where essential avionics, Forward-Looking Infrared (FLIR) sensors, and crew are positioned, disqualifying the possibility of a conventional "tractor" propeller. A pusher-prop is advantageous in its light weight and simplicity. However, the performance of this propulsive device may be improved through the incorporation of cowling.

A ducted fan may be described as a pusher-prop with blades of slightly different geometry, encased by an aerodynamic shroud. While this shroud, known as the "duct," is not articulated, it provides many performance enhancements. Most significantly, the duct may be shaped in such a way that it increases the thrust of the device. Utilizing the cambered shape of an airfoil, the duct manipulates the pressure difference between the inner, ducted flow and external flow of air to provide a boost in thrust capabilities.

Additionally, the duct provides a significant reduction in infrared signature compared to the pusher-prop, which is a highly desirable feature in combat situations. Finally, a ducted fan is safer for the ground crew than a pusher-prop. The spinning blades of the fan are encased and shielded, providing a safety barrier to prevent accidents on the ground.

1.2 Optimization Strategy

Optimization is a strategy often used in the engineering industry to ensure that design decisions are well-informed and robustly aware of why other options were not as satisfactory. This is especially the case in the aerospace engineering industry during the conceptual design of aircraft where most decisions revolve around minimizing an aircraft's weight.

In this investigation, the optimization strategy will be applied to the design of a shrouded propeller. This analysis will be conducted in the form of trade studies to consider various geometries and affirm that rotorcraft's design conditions are satisfied.

CHAPTER 2

DUCTED FAN DESIGN

During early conceptual design of the compound coaxial rotorcraft, it was decided that a 7 ft diameter ducted fan from the experimental Bell-X22A Aircraft would satisfy the offload requirements for the compound portion of the aircraft. This important decision provided a model shrouded propeller to do analysis with and apply to this specific design. The blade characteristics that need to be defined in the following section during the elemental blade analysis will already have been defined in the X-22A documentation, a fortunate discovery whose development is out of the scope of this project.

2.1 Propeller Theory

The following procedure characterizes the propeller portion of the ducted fan through a blade-element theory analysis. It is detailed by Dommasch, Sherby, and Connolly in *Airplane Aerodynamics*.[2] The objective of the operations to be performed in this section is to obtain the propeller thrust and efficiency. Other important physical parameters are listed in Table 2.1 and demonstrated in Figure 2.1.

Table 2.1: Blade Element Theory Parameters

Parameter	Description
T_{req}	required total vehicle thrust, lbs
f_e	total vehicle flat plate drag, ft^2
q	dynamic pressure, psf
c	chord, ft
β	geometric blade angle, deg
ϕ	effective pitch angle, deg
ϕ_0	pitch angle with induced flow, deg
Q	Torque, ft-psf
c_l	coefficient of lift
c_d	coefficient of drag
α_0	$\beta - \phi_0$
θ	induced angle, deg
V_i	induced flow, ft/s
V	forward aircraft speed, ft/s
Ωr	linear velocity due to rotation at station

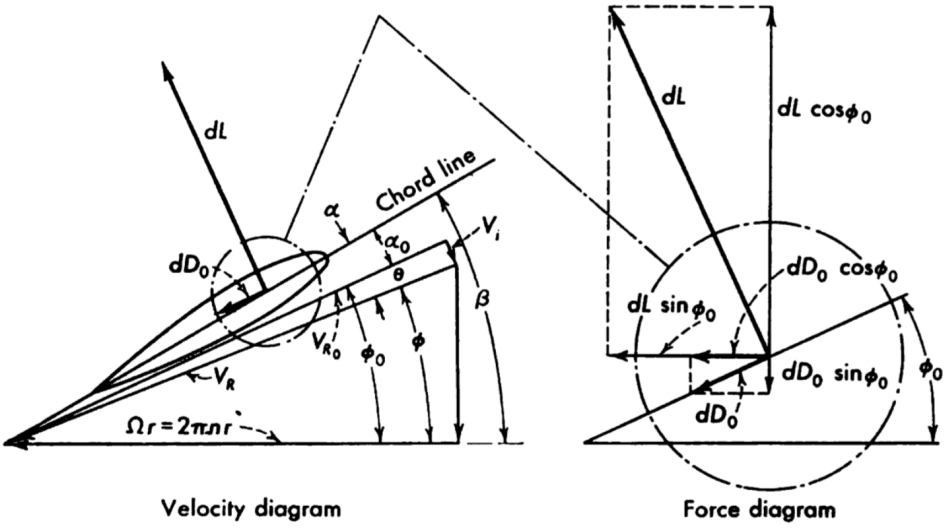

Figure 2.1: Blade Element Theory Physical Representation[2]

The thrust required by the propeller is defined by the following relation:

$$T_{req} = f_e q \qquad \text{Eq. 1}$$

Ultimately, the resulting propeller thrust needs to equal this required thrust, within reasonable geometric bounds. In order to obtain the propeller thrust, several relations need to be calculated and the given blade needs to be characterized for element analysis. Initial fan and shroud sizing are based off the X-22A ducted propeller characterized in the NASA TN D-4142 report.[3]

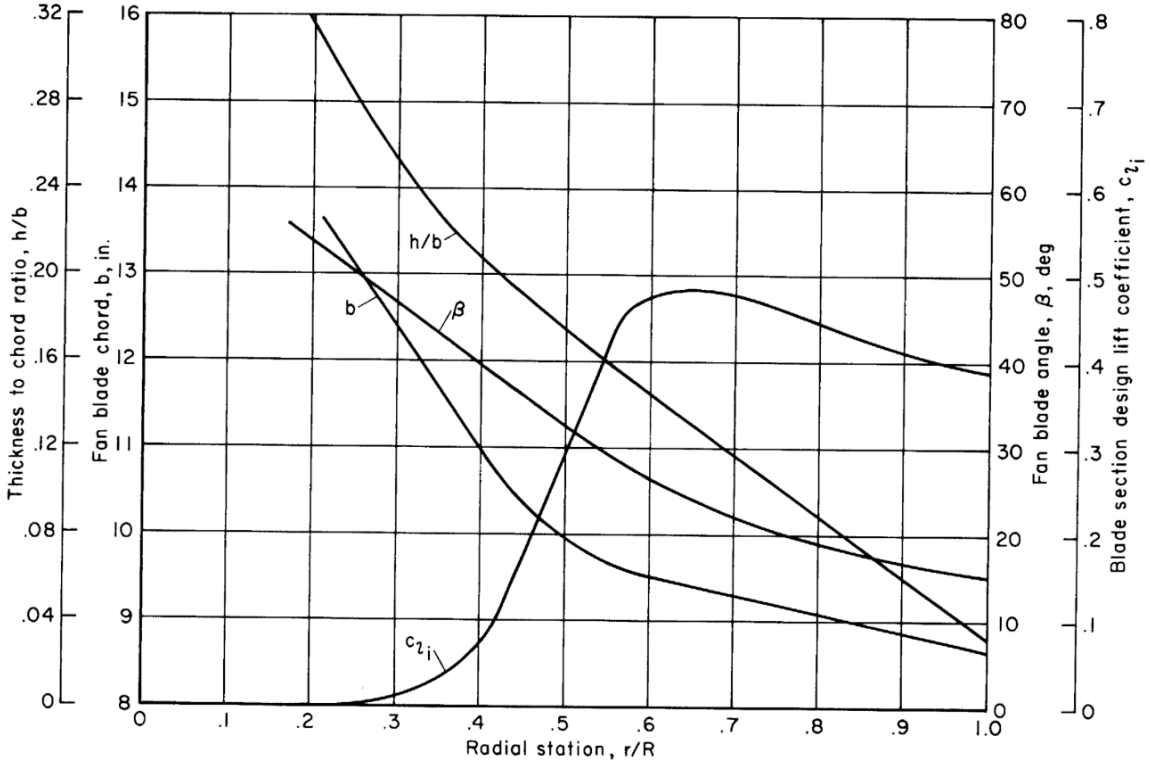

Figure 2.2: X-22 Propeller Blade Characteristics[3]

The following table was populated from the blade characteristics given in Figure 2.2. X station values were arbitrarily, yet carefully selected to capture the trends in both the fan blade chord, b, and the fan blade angle, β.

Table 2.2: Propeller Blade Characteristics

Station, x	0.21	0.25	0.30	0.40	0.45	0.50	0.55	0.60	0.70	0.75	0.80	0.85	0.90	0.95	1.00
Chord	0.57	0.54	0.52	0.46	0.43	0.42	0.41	0.40	0.39	0.38	0.38	0.38	0.37	0.37	0.36
Twist (deg)	57	50	47	40	34	33	29	27	22	20	19	18	17	16	15

Where x is the station of distance from the root of the blade expressed as a normalized value. Starting with the following relation in Eq. 2 for blade solidity:

$$\sigma_R = \frac{Bc}{\pi R} \quad \text{Eq. 2}$$

At any station x, the linear velocity due to rotation is defined by

$$\Omega \text{Rx, where } \Omega = n2\pi \quad \text{Eq. 3}$$

the geometric blade angle is defined by

$$\beta = twist + \beta_{75^o} \quad \text{Eq. 4}$$

the effective pitch angle is defined by

$$\phi = \tan^{-1}\left(\frac{V}{\pi n D x}\right) \quad \text{Eq. 5}$$

and the induced angle is defined by

$$\theta = \frac{\beta - \phi}{1 + \frac{8x\sin(\phi)}{\sigma_R a_0}} \quad \text{Eq. 6}$$

where the lift coefficient is represented by

$$c_l = a_0(\beta - \phi - \theta) \quad \text{Eq. 7}$$

Now, allowing the following:

$$\lambda_T = \frac{\cos^2(\theta)}{\cos^2(\phi)}(c_l \cos(\phi) - c_d \sin(\phi_0) \quad \text{Eq. 8}$$

$$\lambda_Q = \frac{\cos^2(\theta)}{\cos^2(\phi)}(c_l \sin(\phi_0) - c_d \cos(\phi_0)) \quad \text{Eq. 9}$$

where

$$dT = \frac{\rho}{2}(2\pi n)^2 bBR^3 x^2 dx\, \lambda_T \quad \text{Eq. 10}$$

$$dQ = \frac{\rho}{2}(2\pi n)^2 bBR^4 x^3 dx\, \lambda_Q \quad \text{Eq. 11}$$

and

$$\frac{dCt}{dx} = 3.88\, x^2 \sigma_R \lambda_T \quad \text{Eq. 12}$$

$$\frac{dCQ}{dx} = 1.94\, x^3 \sigma_R \lambda_Q \quad \text{Eq. 13}$$

Eq. 12 and Eq. 13 be numerically integrated throughout the x station vector. Once integrated, the following relations are applicable, resulting in thrust and torque felt by the propeller.

$$T = C_T \rho n^2 D^4 \quad \text{Eq. 14}$$

$$Q = C_Q \rho n^2 D^5 \quad \text{Eq. 15}$$

2.2 Duct Theory

The method utilized to do initial sizing for the duct, or shroud, around the fan closely follows that of the shroud characterization in *An Aerodynamic Analysis of Ducted Tail Rotors* by Batra.[4] The objective of this procedure is to determine the thrust on the duct itself, requiring the radial velocity at the quarter chord and the circulation in the vortex ring be determined. This analysis is performed under the approximation that all of the circulation distribution throughout the duct can be replaced by a vortex ring at the quarter (¼) chord of the duct's shroud. This vortex's strength then can be determined by satisfying the flow boundary conditions at the ¾ chord duct location. The solution for circulation can then be utilized to solve for the shroud's thrust. The following Table 2.3 contains important parameters to be introduced in this section.

Table 2.3: Duct Important Parameters

Parameter	Description
r	radial distance, ft
z	distance from propeller, ft
R_p	duct radius at propeller, ft
R_z	duct radius at point z, ft
V	velocity, ft/s
w_o	axial velocity at propeller, ft/s
w_z	Axial velocity at z, ft/s
ϕ_0	pitch angle with induced flow, deg
Γ	flow circulation strength

From the following figure from Batra, illustrating a streamtube around a thrusting rotor, it is important to note the physical locations at which axial velocity components will be modeled from momentum theory.

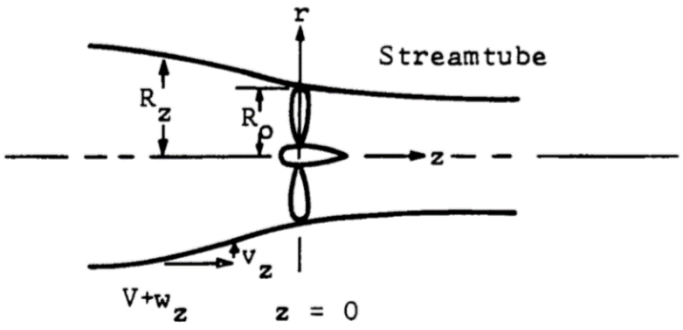

Figure 2.3: Streamtube around Thrusting Rotor[4]

At z = 0, the axial flow velocity component is expressed by the following relation:

$$w_o = \frac{1}{2}\left(-V + \left(V^2 + \frac{2T_R}{\rho\pi R_o^2}\right)^{\frac{1}{2}}\right) \qquad \text{Eq. 16}$$

At another location where z is nonzero, this axial velocity is expressed by

$$w_z = w_o\left(1 + \frac{z}{\sqrt{R_o^2 + z^2}}\right) \quad \text{Eq. 17}$$

From mass flow continuity, it is known that

$$\dot{m} = \rho\pi R_o^2(V + w_o) = \rho\pi R_z^2(V + w_z) \quad \text{Eq. 18}$$

Rearranging Eq. 18 results in the following relation for the radius of the streamtube where z is not zero.

$$R_z^2 = \frac{R_o^2(V + w_o)}{(V + w_z)} \quad \text{Eq. 19}$$

The slope of the streamtube can then be approximated with small angle assumption, where $\tan(\theta) \approx \theta$, and is shown in Eq. 20.

$$\theta = \frac{dR_z}{dz} = \frac{v_z}{(V + w_z)} \quad \text{Eq. 20}$$

Differentiating Eq. 19 and then substituting into Eq. 20,

$$\frac{dR_z}{dz} = \frac{-R_z}{2(V + w_z)}\frac{dw_z}{dz} \quad \text{Eq. 21}$$

And similarly differentiating Eq. 17

$$\frac{dw_z}{dz} = \frac{+w_o R_o^2}{(R_o^2 + z^2)^{\frac{3}{2}}} \quad \text{Eq. 22}$$

And now substituting both Eq. 21 and Eq. 22 into Eq. 20 results in the radial velocity at any location where z is non zero:

$$v_z = \frac{-w_o R_o^2 R_z}{2(R_o^2 + z^2)^{\frac{3}{2}}} \quad \text{Eq. 23}$$

The following figure demonstrates the boundary condition at the quarter chord of the shroud.

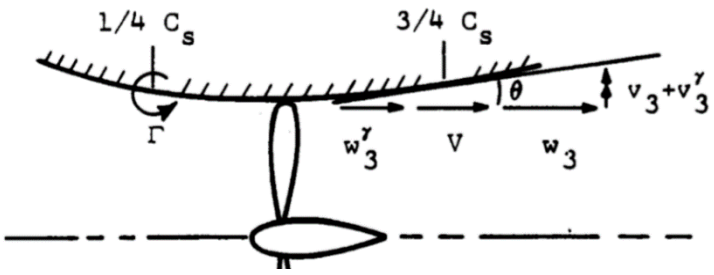

Figure 2.4: 3/4 Chord Boundary Condition[4]

Upon satisfying the flow condition at the ¾ chord, the circulation strength of the vortex ring being modeled through the duct can be determined. The relation that satisfies the flow condition is included below in Eq. 24 and the resulting circulation is further expanded to equation Eq. 25.

$$\Gamma = \frac{-2\pi R_l v_3^\gamma}{f_r} \qquad \text{Eq. 24}$$

$$\Gamma = \frac{-2\pi R_l}{f_r}(\theta(V + w_3) - v_3) \qquad \text{Eq. 25}$$

The shroud thrust can now be calculated utilizing the following relation for the generalized circulation strength solution:

$$\mathrm{T_s} = \frac{\rho v_1 (2\pi R_l)^2}{f_r}(\theta(V + w_3) - v_3) \qquad \text{Eq. 26}$$

Where the parameter f_r was determined with Figure 2.5 at the corresponding radius ratio and duct chord to diameter ratio.

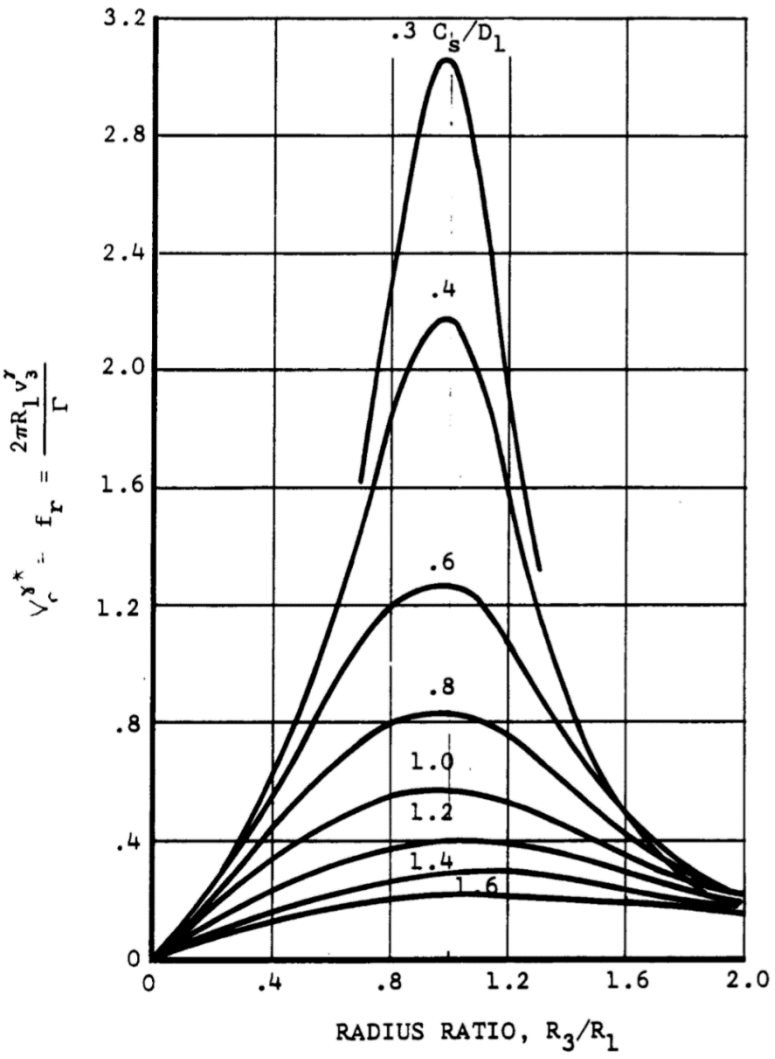

Figure 2.5: Radial Velocity Inducted at 3/4 Chord by a Vortex Ring at 1/4 Chord[4]

This graph was digitized into close-fit higher order polynomials in order to programmatically read the graphical data. The corresponding coefficients are found in the Appendix B within the Ducted Fan MATLAB program.

CHAPTER 3

OPTIMIZATION METHODOLOGY

From the procedures outlined in the previous section, two MATLAB programs were created to converge on design solutions based on initial propeller and shroud design parameters. Once the programs were functioning independently, they were fitted to run for a variety of trade points in preparation for a trade study. The propeller program was created with the intention to provide the configuration which provided the greatest amount of thrust, with the smallest amount of torque, at the lightest weight. The duct trade study was solely run to find the smallest weight possible for the ducted fan in its entirety. The trade studies compared different blade numbers and duct/fan geometries to attempt to find an observable trend in performance that could highlight the most optimal combination of design parameters.

3.1 Propeller Trade Study

The propeller trade study program was iterated for fan diameters of 3 to 6 ft in increments of 0.5 ft, and blade counts of 4 to 6 blades. These are all reasonable values considered in industry for light aircraft and considered for the conceptual design of the ducted fan. For each combination of fan diameter and blade counts, the propeller procedure needed to converge to a solution for $\beta_{@.75}$, the twist at 75% of the length of the blade. It is important to note this value cannot exceed 90 degrees, therefore solutions outside of physical credibility are not able to be considered.

3.2 Ducted Fan Trade Study

The ducted fan trade study is a geometrical approach to determine a minimum weight combination of design parameters. Blades were again varied from 4 to 10 blades, fan diameter was varied from 3 to 6 ft, and duct chord to fan diameter ratio was varied from 0.4 to 1.6, in increments of 0.2. For each of the three parameter combinations, the duct sizing procedure was performed, and then the propeller model was additionally allowed to converge to a thrust solution.

CHAPTER 4

RESULTS

4.1 Propeller Trade Study

In this study, Torque experience by the propeller is a parameter that is desired to be driven as low as possible. A fan that produces lower torque can be designed lighter; therefore, the objective of this assertion is the need to be consistently making the vehicle lighter. It was discovered that fan diameters lower than 4 ft tend to require the 0.75β twist angle exceed the physical limit of 90 degrees; therefore those diameters were not found to be viable solutions. The following figures 4.1, 4.2, and 4.3 consist of cheater plots with constant fan diameter lines, increasing blade counts, and Torque relationships.

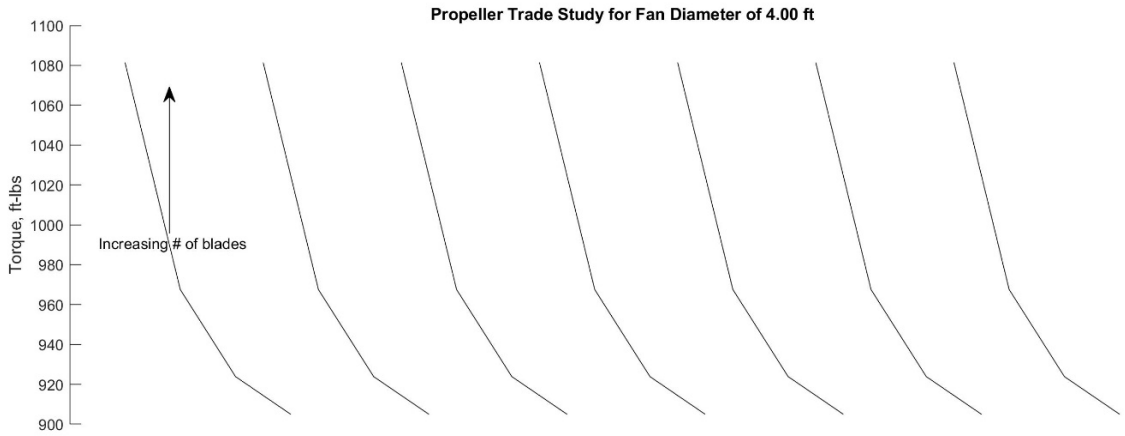

Figure 4.1: Diameter of 4 ft, Variable blade, Torque Cheater Plots

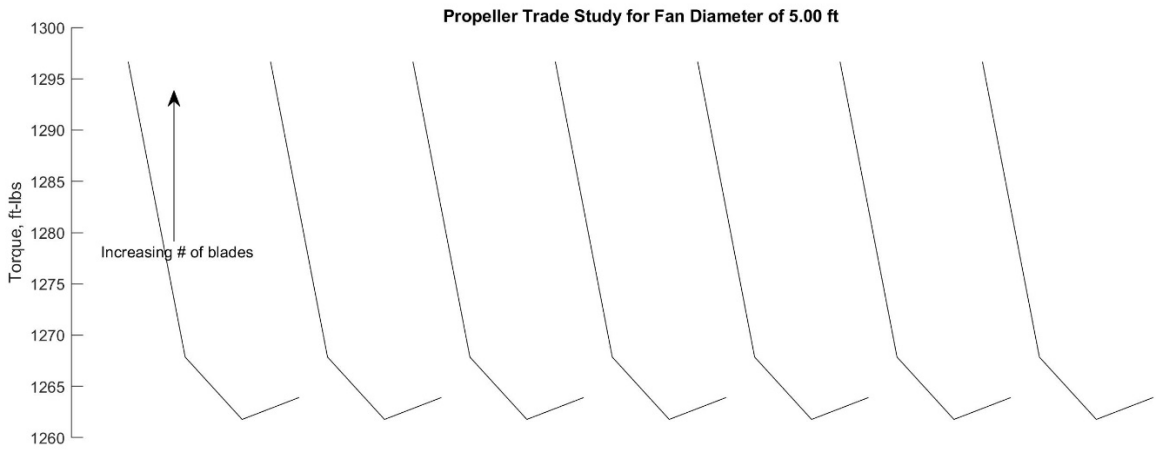

Figure 4.2: Diameter of 5 ft, Variable blade, Torque Cheater Plots

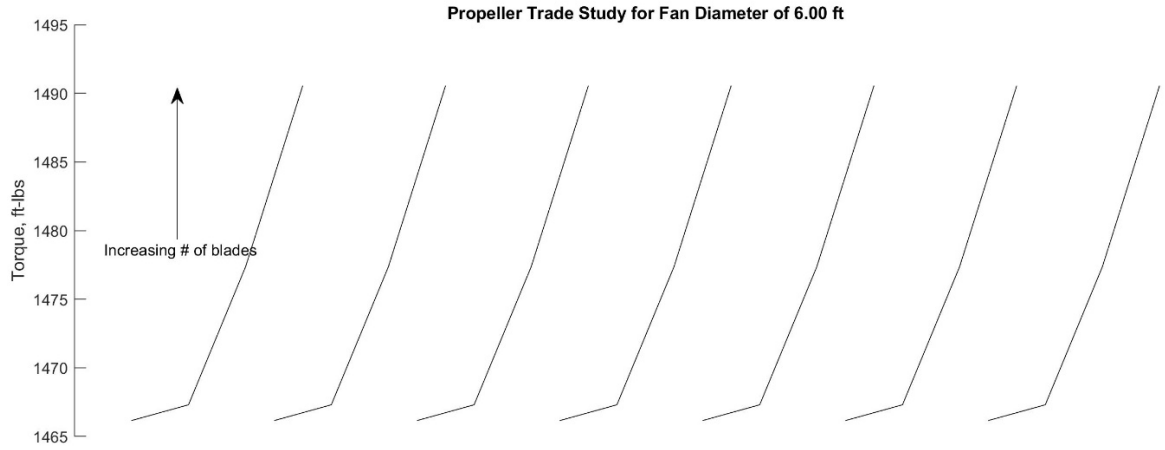

Figure 4.3: Diameter of 6 ft, Variable blade, Torque Cheater Plots

A clear and expected result from these cheater plots is as blade count increases, Torque increases. A higher blade count can increase propeller efficiency and thrust, but the structure will compensate in weight as the torque produced by the system increases. The minimum torque combinations desirable from this trade study were any blade combination with a 4 feet diameter fan, or 5 blades and a 5 ft diameter fan.

4.2 Ducted Fan Trade Study

The parameters at the focus of this study were the blade count, fan diameter, and duct chord to fan diameter ratio to observe their effect on the total weight of the ducted fan. The following figure from the trade study was conducted for a fan diameter of 3 ft.

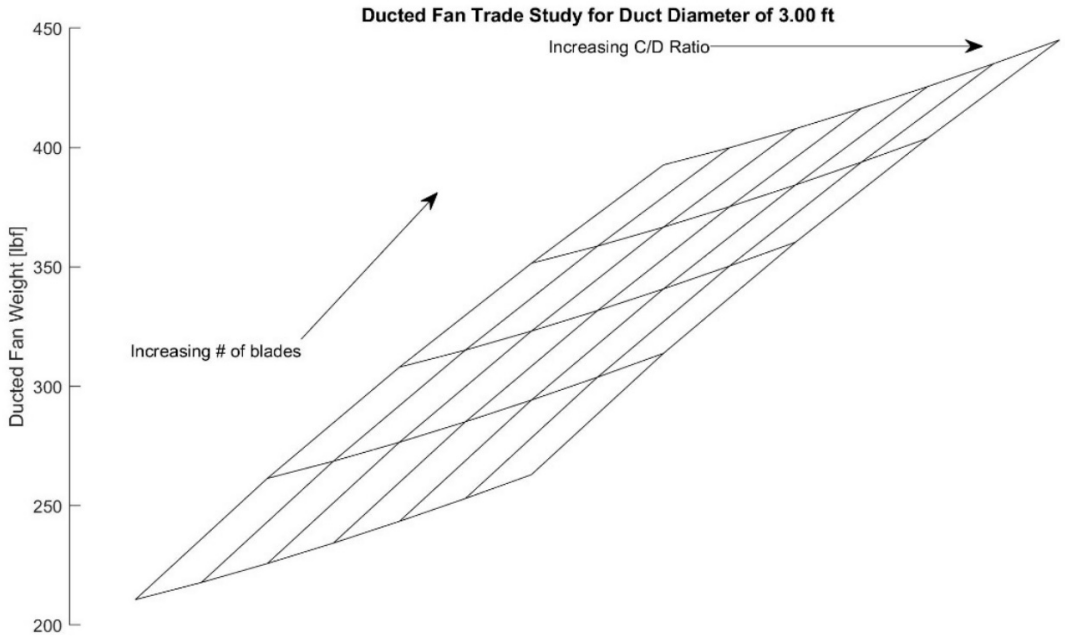

Figure 4.4: 3 ft Diameter Duct Trade Study

It was discovered during the propeller trade study section that a fan with a diameter less than four feet was unable to converge to a viable blade twist solution; therefore, this first cheater plot cannot provide conclusive results. The remaining graphs included below confirm a clear and expected direct relationship with increasing blades, increasing duct chord to fan diameter ratio also result in an increased weight.

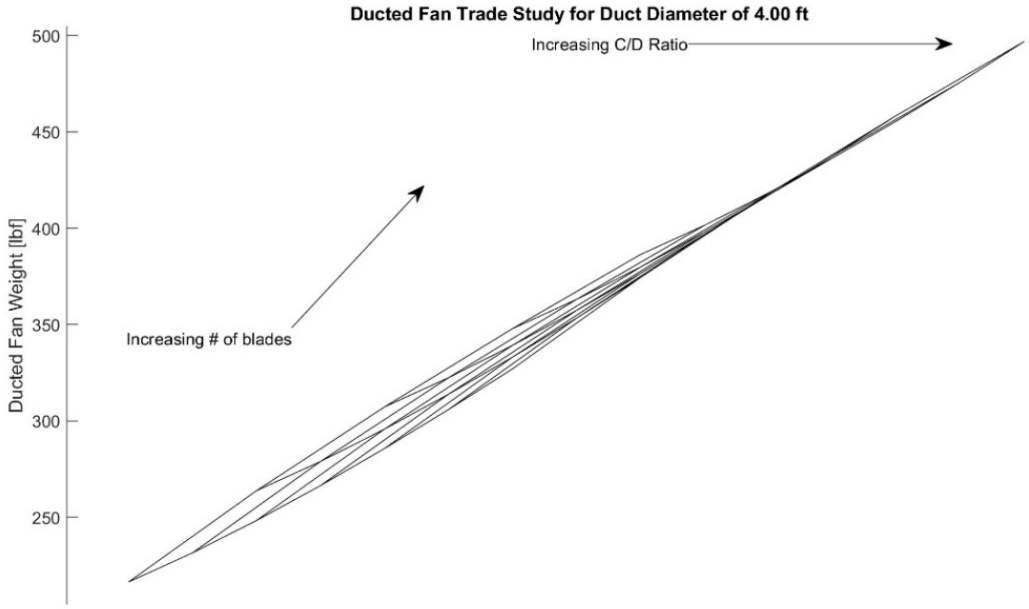

Figure 4.5: 4 ft Diameter Duct Trade Study

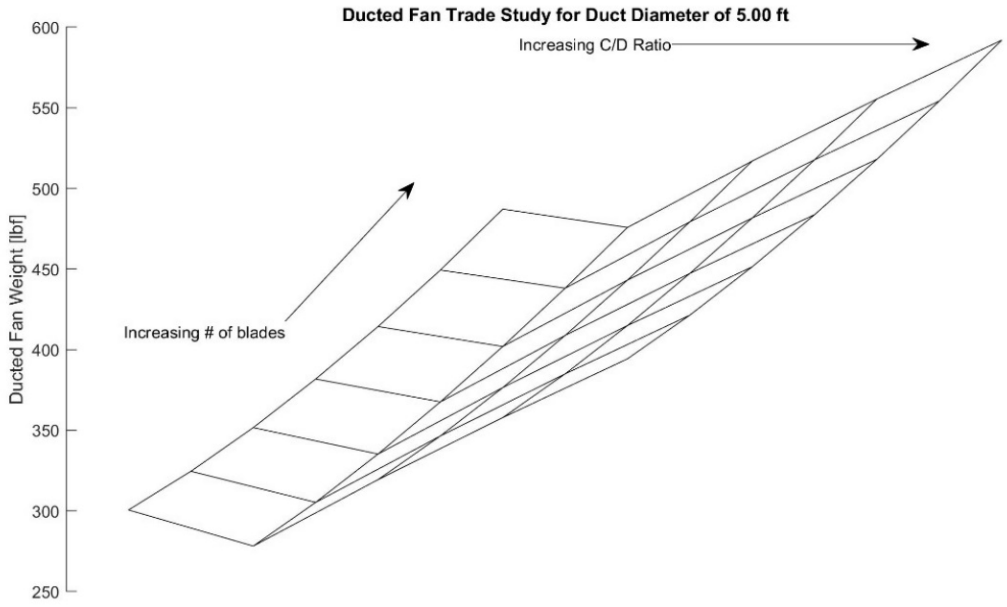

Figure 4.6: 5 ft Diameter Duct Trade Study

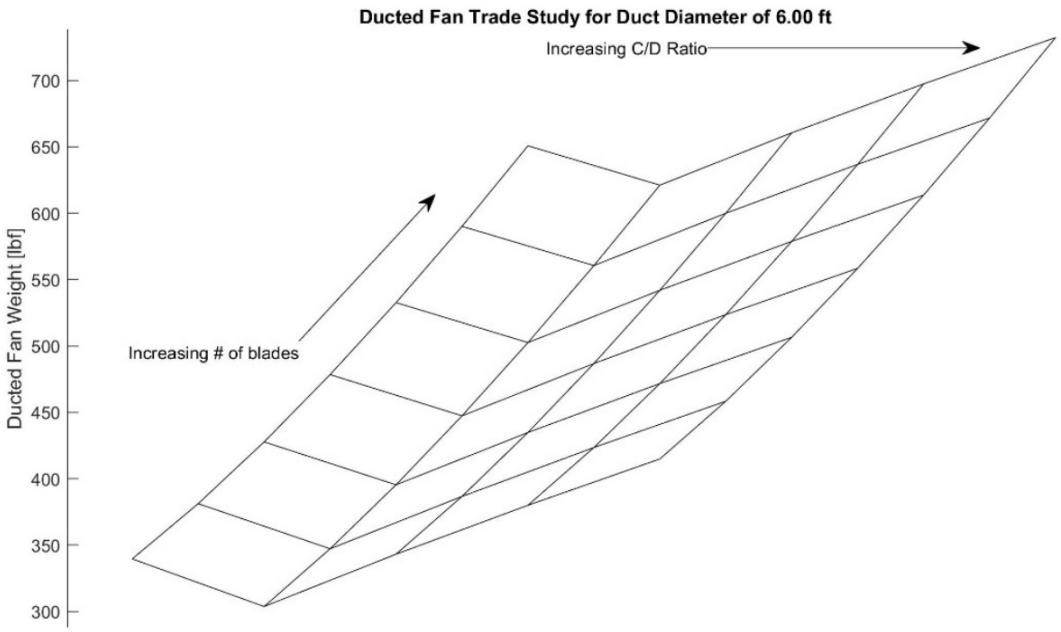

Figure 4.7: 6 ft Diameter Duct Trade Study

From all three of the remaining figures however, there is a distinct trough where a parameter combination consistently provided a lower ducted fan weight. The furthest left solutions are constant lines of duct chord/diameter ratio. When this value is closest to 1, the ducted fan behaves ideally, therefore the lowest weight solutions may not be realistic solutions and must be further investigated before selecting.

These observable trends can be compared to the optimal parameters obtained in the propeller trade study, where lower blade count and diameter are favorable in this case of lowered torque. This study concluded that a smaller diameter, less blade count ducted fan was lighter and affirmed that the previous discovered solution of five blades at a five ft diameter fan was the smallest weight solution in Figure 4.6.

CHAPTER 5

CONCLUSION

An investigation was conducted on a ducted fan to optimally size the propeller and shroud. For the FARA mission, designing an aircraft to be as lightweight as possible is crucial to being able to reach the high speeds in the flight envelope. In the addition of an auxiliary ducted fan, it was imperative to size the ducted fan to be as small as possible without sacrificing performance.

Based on the trade study results, the recommended number of blades and fan diameter is five blades and 5 ft, respectively. That being said, the final differences between 4 and 5 ft diameter duct weights or between 5 and 6 ft diameter weights are not very large in magnitude. The resulting duct diameter has the freedom to then be sized according to a required thrust if the smallest configuration does not produce the required amount of total thrust.

APPENDIX A

PROPELLER PROGRAM

```
%% Propeller Program
%Objective is to sweep D and B to satisfy design conditions and minimize Torque
Dvec = 3:0.5:6;                          %DIAMETER, FT
Bvec = [4 5 6 7];                        %BLADES
RPM = 4399;                              %RPM FORWARD FLIGHT

fe = 20.4920;                            % FLAT PLATE DRAG FROM DRAG MODULE AT
                                 %DASH [ft^2]
atmos = usstdatmos(5000);                % CRUISE CONDITION AMBIENT
rho = atmos.rho;                         % CRUISE ALTITUDE DENSITY [SLUG/FT^3]
a = atmos.a;                             % CRUISE ALTITUDE SPEED OF SOUND [FT/SEC]
V = 200*1.68781;                         % DESIGN VELOCITIY (Cruise) [ft/s]
q = 0.5*rho*(V^2);                       % DYNAMIC PRESSURE [PSF]

T = fe*q;                                % THRUST REQUIRED [lb_f]
n_p = 0.95;                              % PROP EFFICIENCY
HP  = T*V/(n_p*550);                     % HORSEPOWER REQUIRED [hp]
grid = 0;

x = [0.210 0.250 0.300 0.400 0.450 0.500 0.550 0.600 0.700 0.750 0.800 0.850 0.900 0.950
1.000];
a0 = 0.1*180/pi;
x2 = x.^2;
x3 = x.^3;
chord = [13.700 13.000 12.400 11.000 10.400 10.000 9.750 9.700 9.300 9.200 9.100        9.000
8.900 8.800 8.700];
beta75 = 0;
twist = [57.000 50.000 47.000 40.000 34.000 33.000 29.000 27.000 22.000 20.00019.000 18.000
          17.000  16.000  15.000]; %BLADE ANGLE, DEG
%% Solution
for ii = 1:length(Dvec)
   D = Dvec(ii);
   count = 0;
   grid = grid+1;
   for jj = 1:length(Bvec)
      beta75 = 0;
      B = Bvec(jj);
      chord = [13.700      13.000 12.400 11.000 10.400 10.000 9.750 9.700 9.300 9.200
          9.100 9.000 8.900 8.800 8.700];
      chord = chord/(D*12/2);
      sigma = B*chord/(pi*D/2);
      T_prop = 0;
      while abs(T_prop-T) > 10
         Omega = RPM*2*pi/60;
         omegaRx = Omega*D/2*x;
         for i=1:length(x)
            beta(i) = twist(i) + beta75;
            phi(i) = atan(V/(pi*RPM/60*D*x(i))); %rad
            phi_d(i) = phi(i)*180/pi;
            theta(i) = (beta(i)-phi_d(i))/(1+8*x(i)*sin(phi(i))/sigma(i)/a0);
         end
```

```
        phi_0 = phi_d-theta;
        alpha_0 = beta-phi_d-theta;
        cl0 = alpha_0 *0.1;
        for i=1:length(cl0)
           cd(i) = 0.0062737*(cl0(i)^4) - 0.006392*(cl0(i)^3) + 0.0058475*(cl0(i)^2) +
         0.00015828*(cl0(i)) + 0.01499;
           lambda_t(i) =
         (cos(theta(i)*pi/180))^2/(cos(phi(i)))^2*(cl0(i)*cos(phi_0(i)*pi/180)-
         cd(i)*sin(phi_0(i)*pi/180));
           lambda_q(i) =
         (cos(theta(i)*pi/180))^2/(cos(phi(i)))^2*(cl0(i)*sin(phi_0(i)*pi/180)+cd(i)*cos(ph
         i_0(i)*pi/180));
           dCtdx(i) = 3.88*x2(i)*sigma(i)*lambda_t(i);
           dCqdx(i) = 1.94*x3(i)*sigma(i)*lambda_q(i);
        end

        J = V/(RPM/60*D);
        Ct = 0;    Cq = 0;
        for i = 1:(length(x)-1)
           Ct = Ct + (x(i+1)-x(i))*dCtdx(i);
           Cq = Cq + (x(i+1)-x(i))*dCqdx(i);
        end
        Cp = 2*pi*Cq;
        eta_prop = Ct*V/(Cp*RPM/60*D);
        T_prop = Ct*rho*(RPM/60)^2*D^4;
        Q_prop = Cq*rho*(RPM/60)^2*D^5;
        beta75 = beta75 + .001;
     end
     trade_point = [B, D, beta75, Q_prop];
     count = count+1;
     prop_trade(count,1:4,grid) = trade_point;
  end
end
%% Data Processing
for ii = 1:length(Dvec)
  for jj = 1:length(Bvec)
     [idx,~]=find(prop_trade(:,1,ii)==Bvec(jj));
     prop_carpet(jj,:,ii)=prop_trade(idx,4,ii);
  end
  figure(),carpet(Bvec,Dvec,prop_carpet(:,:,ii)',5);
  ylabel('Torque, ft-lbs')
  name = sprintf('Propeller Trade Study for Fan Diameter of %0.2f ft',Dvec(ii));
  title(name)
  annotation('textarrow',[0.2,0.2],[0.5,.8],'String','Increasing # of blades')
  hold on
end
```

APPENDIX B

DUCT PROGRAM

```
%%Ducted Fan Program
%% Ambient Conditions
atmos = usstdatmos(8000);              % CRUISE CONDITION AMBIENT
rho = atmos.rho;                       % CRUISE ALTITUDE DENSITY [SLUG/FT^3]
a = atmos.a;                           % CRUISE ALTITUDE SPEED OF SOUND [FT/SEC]
V   = 170*1.68781; %Velocity           % DESIGN VELOCITIY (Cruise) [ft/s]
M = V/a;                               % CRUISE CONDITION MACH NUMBER []
q = 0.5*rho*(V^2);                     % DYNAMIC PRESSURE [PSF]

%% Iteration Variables
%{
Shroud diameter
Shroud chord to diameter ratio
Number of propeller blades
%}

%% Other Constants
n_p = 0.95;                            % PROPELLER EFFICIENCY

%% Thrust and Power Requirements
fe.total = 21.3551; %at cruise
T   = fe.total*q;                      % THRUST REQUIRED [lb_f]
HP  = T*V/(n_p*550);                   % HORSEPOWER REQUIRED [hp]

%% Initialization
grid = 0;
Diavec = 3:1:6;
CsDvec = 0.4:0.2:1.6;
Bvec = 5:2:10;

%% Calculation Loop
for ii = 1:length(Diavec)
   Dia = Diavec(ii);
   count = 0;
   grid = grid+1;
   for jj = 1:length(CsDvec)
      CsD = CsDvec(jj);
      for kk = 1:length(Bvec)
         B = Bvec(kk);
         Cs  = CsD*Dia;                % SHROUD CHORD MATRIX, ft
         z_1 = Cs*-0.25;               % 1/4 CHORD STATION, ft
         z_3 = Cs*0.25;                % 3/4 CHORD STATION, ft
      %% Axial Velocities
         w_o = 0.5*(-V + sqrt(V^2 + (2*T)/(rho*pi*(Dia/2)^2)));    % V_AXIAL  DUCT, ft/s
         w_1 = w_o*(1+(z_1/sqrt((Dia/2)^2+z_1^2)));                % V AXIAL 1/4 CHORD, ft/s
         w_3 = w_o*(1+(z_3/sqrt((Dia/2)^2+z_3^2)));                % V AXIAL 3/4 CHORD, ft/s
      %% Stream Tube
         R_1 = sqrt((Dia/2)^2*(V+w_o)/(V+w_1));                    % STREAM TUBE R AT 1/4
CHORD, ft
         R_3 = sqrt((Dia/2)^2*(V+w_o)/(V+w_3));                    % STREAM TUBE RADIUS
AT 3/4 CHORD [ft]
```

```
    %% Radial Velocity
      v_1 = (-w_o*(Dia/2)^2*R_1)/(2*((Dia/2)^2+z_1^2)^(3/2));        % RADIAL
VELOCITY AT 1/4 CHORD [ft/s]
      v_3 = (-w_o*(Dia/2)^2*R_3)/(2*((Dia/2)^2+z_3^2)^(3/2));        % RADIAL
VELOCITY AT 3/4 CHORD [ft/s]
    %% Diffuser Geometry
      A_3 = v_3/(V+w_3);                % DIFFUSER ANGLE AT 3/4 CHORD
      v3g = A_3*(V+w_3)+v_3;          % INDUCED RADIAL VELOCITY 3/4 CHORD [ft/s]

      CsD1 = Cs/(R_1* 2);               % CHORD / D_1 RATIO
      R3_1 = R_3/R_1;                   % RADIUS RATIO
    %% Solution
      if CsD1 <= 0.4
        f_r = (-46.29919607)*R3_1^6 + (280.98525274)*R3_1^5 +...
          (-671.65156471)*R3_1^4 + (802.64433516)*R3_1^3 +...
          (-505.75257769)*R3_1^2 + (162.67570593)*R3_1 +...
          (-20.43480100);

      elseif CsD1 > 0.4 && CsD1 < 0.6
        f_r_low = (-46.29919607)*R3_1^6 + (280.98525274)*R3_1^5 +...
          (-671.65156471)*R3_1^4 + (802.64433516)*R3_1^3 +...
          (-505.75257769)*R3_1^2 + (162.67570593)*R3_1 +...
          (-20.43480100);
        f_r_high = (-1.94258175)*R3_1^6 + (11.14338239)*R3_1^5 +...
          (-22.53863883)*R3_1^4 + (18.44224759)*R3_1^3 +...
          (-5.69523210)*R3_1^2 + (1.86467001)*R3_1 +...
          (-0.00158957);
        f_r = ((0.6 - CsD1)*f_r_low + (CsD1 - 0.4)*f_r_high)/0.2;

      elseif CsD1 == 0.6
        f_r = (-1.94258175)*R3_1^6 + (11.14338239)*R3_1^5 +...
          (-22.53863883)*R3_1^4 + (18.44224759)*R3_1^3 +...
          (-5.69523210)*R3_1^2 + (1.86467001)*R3_1 +...
          (-0.00158957);

      elseif CsD1 > 0.6 && CsD1 < 0.8
        f_r_low = (-1.94258175)*R3_1^6 + (11.14338239)*R3_1^5 +...
          (-22.53863883)*R3_1^4 + (18.44224759)*R3_1^3 +...
          (-5.69523210)*R3_1^2 + (1.86467001)*R3_1 +...
          (-0.00158957);
        f_r_high = (-0.10599293)*R3_1^5 + (1.13041047)*R3_1^4 +...
          (-3.13620283)*R3_1^3 + (2.38066276)*R3_1^2 +...
          (0.54509114)*R3_1 + (0.02304480);
        f_r = ((0.8 - CsD1)*f_r_low + (CsD1 - 0.6)*f_r_high)/0.2;

      elseif CsD1 == 0.8
        f_r = (-0.10599293)*R3_1^5 + (1.13041047)*R3_1^4 +...
          (-3.13620283)*R3_1^3 + (2.38066276)*R3_1^2 +...
          (0.54509114)*R3_1 + (0.02304480);

      elseif CsD1 > 0.8 && CsD1 < 1.0
```

```
    f_r_low = (-0.10599293)*R3_1^5 + (1.13041047)*R3_1^4 +...
       (-3.13620283)*R3_1^3 + (2.38066276)*R3_1^2 +...
       (0.54509114)*R3_1 + (0.02304480);
    f_r_high = (-0.02417088)*R3_1^5 + (0.41149876)*R3_1^4 +...
       (-1.22632951)*R3_1^3 + (0.70622716)*R3_1^2 +...
       (0.69397891)*R3_1 + (0.02034047);
    f_r = ((1.0 - CsD1)*f_r_low + (CsD1 - 0.8)*f_r_high)/0.2;

elseif CsD1 == 1.0
    f_r = (-0.02417088)*R3_1^5 + (0.41149876)*R3_1^4 +...
       (-1.22632951)*R3_1^3 + (0.70622716)*R3_1^2 +...
       (0.69397891)*R3_1 + (0.02034047);

elseif CsD1 > 1.0 && CsD1 < 1.2
    f_r_low = (-0.02417088)*R3_1^5 + (0.41149876)*R3_1^4 +...
       (-1.22632951)*R3_1^3 + (0.70622716)*R3_1^2 +...
       (0.69397891)*R3_1 + (0.02034047);
    f_r_high = (0.03274858)*R3_1^5 + (-0.03808270)*R3_1^4 +...
       (-0.16083046)*R3_1^3 + (-0.03880374)*R3_1^2 +...
       (0.59446575)*R3_1 + (0.01952454);
    f_r = ((1.2 - CsD1)*f_r_low + (CsD1 - 1.0)*f_r_high)/0.2;

elseif CsD1 == 1.2
    f_r = (0.03274858)*R3_1^5 + (-0.03808270)*R3_1^4 +...
       (-0.16083046)*R3_1^3 + (-0.03880374)*R3_1^2 +...
       (0.59446575)*R3_1 + (0.01952454);

elseif CsD1 > 1.2 && CsD1 < 1.4
    f_r_low = (0.03274858)*R3_1^5 + (-0.03808270)*R3_1^4 +...
       (-0.16083046)*R3_1^3 + (-0.03880374)*R3_1^2 +...
       (0.59446575)*R3_1 + (0.01952454);
    f_r_high = (0.07358044)*R3_1^5 + (-0.29056422)*R3_1^4 +...
       (0.34581729)*R3_1^3 + (-0.31719322)*R3_1^2 +...
       (0.47887681)*R3_1 + (0.01021639);
    f_r = ((1.4 - CsD1)*f_r_low + (CsD1 - 1.2)*f_r_high)/0.2;

elseif CsD1 == 1.4
    f_r = (0.07358044)*R3_1^5 + (-0.29056422)*R3_1^4 +...
       (0.34581729)*R3_1^3 + (-0.31719322)*R3_1^2 +...
       (0.47887681)*R3_1 + (0.01021639);

elseif CsD1 > 1.4 && CsD1 < 1.6
    f_r_low = (0.07358044)*R3_1^5 + (-0.29056422)*R3_1^4 +...
       (0.34581729)*R3_1^3 + (-0.31719322)*R3_1^2 +...
       (0.47887681)*R3_1 + (0.01021639);
    f_r_high = (-8.1196613775E-02)*R3_1^5 + (4.4023027354E-01)*R3_1^4      +...
       (-8.0824605727E-01)*R3_1^3 + (4.2009597443E-01)*R3_1^2 +...
       (2.4775077746E-01)*R3_1 + (6.5049118529E-03);
    f_r = ((1.6 - CsD1)*f_r_low + (CsD1 - 1.4)*f_r_high)/0.2;

else
```

```
            f_r = (-8.1196613775E-02)*R3_1^5 + (4.4023027354E-01)*R3_1^4 +...
              (-8.0824605727E-01)*R3_1^3 + (4.2009597443E-01)*R3_1^2 +...
              (2.4775077746E-01)*R3_1 + (6.5049118529E-03);
         end

      %% Duct Thrust and Weight Calculations
         Cir = (-2*pi()*R_1*v3g)/f_r;                    % CIRCULATION STRENGTH
         T_s = rho*v_1*(-2*pi()*R_1)*Cir;                % SHROUD THRUST [lb_f]
         S_d = pi*((0.44*(Dia/2))+ Dia)*0.9*Cs;          % DUCT WETTED AREA [ft^2]
         Wn = 0.03*sqrt(V/1.68781)*(S_d^1.3);            % NACELLE WEIGHT [lb_m]

      %% Iterative Propeller Analysis
         Vtip = 700;                                     % INITIAL VALUE FOR CONVERGENCE
         Tprop = 0;                                      % INITAL VALUE FOR CONVERGENCE
         while T-(Tprop+T_s)>1
            Vtip = Vtip+1;
            rpm = Vtip*60/(pi*Dia);
            [Tprop] = propeller_v3(Dia,B,rpm);
         end
      %% Propeller Weight
         Wp =
100*((Dia/10)^2+(B/4)^0.7*(150/100)^0.75*(rpm*Dia/20000)^0.5*(M+1)^0.5*(HP/(10*Dia^2))
^0.12);
         Wd = Wp+Wn;                                     % DUCTED FAN WEIGHT [lb_m]
         TW = T/Wd;                                      % THRUST TO WEIGHT RATIO
         trade_point = [B, CsD, Vtip, rpm, TW, Wd];
         count = count+1;
         ducted_fan_trade(count,1:6,grid) = trade_point;
      end
   end
end

%% Data Processing
for ii = 1:length(Diavec)
   for jj = 1:length(Bvec)
      [idx,~]=find(ducted_fan_trade(:,1,ii)==Bvec(jj));
      ducted_fan_carpet(jj,:,ii)=ducted_fan_trade(idx,6,ii);
   end
   figure(),carpet(Bvec,CsDvec,ducted_fan_carpet(:,:,ii)',5);
   ylabel('Ducted Fan Weight [lbf]')
   name = sprintf('Ducted Fan Trade Study for Duct Diameter of %0.2f ft',Diavec(ii));
   title(name)
   annotation('textarrow',[0.3,0.4],[0.5,0.7],'String','Increasing # of blades')
   annotation('textarrow',[0.6,0.8],[0.9,0.9],'String','Increasing C/D Ratio')
   hold on
end
```

REFERENCES

[1] “Program Solicitation for Future Attack Reconnaissance Aircraft (FARA) Competitive Prototype,” US Army Contracting Command – Redstone, Solicitation Number W911W6-19-R-0001.

[2] Dommasch, D. O., Sherby, S. S., and Connolly, T., *Airplane Aerodynamics 3rd Ed*., Pitman Publishing, 1961.

[3] Mort, K. W., Gamse, B. “A Wind Tunnel Investigation of a 7ft Diameter Ducted Propeller” NASA TN D-4142, Washington, 1967.

[4] Batra, N. N., “An Aerodynamic Analysis of Ducted Tail Rotors,” Bell Helicopter Company, Report No. 599-181-902, 1971.

[5] “Preliminary Design II & Synthesis Compound Coaxial Helicopter” MAE 4351-003 Aerospace Vehicle Design 2, Spring 2020.

BIOGRAPHICAL INFORMATION

Anna studied Aerospace Engineering at The University of Texas at Arlington (UTA), starting in 2016 and has been involved in many projects since then, the most interesting of which is involvement in the resurrection of the UTA Student Unmanned Aerial Systems team the fall of 2019. After learning of the international SUAS competition through the Unmanned Vehicle Systems certificate program, Anna found classmates that were willing to devote countless hours to putting together an autonomous RC platform to compete. As the Spring 2020 social distancing guidelines prevented the team from being able to compete, Anna focused on finishing her degree, starting her masters through the fast-track program, and focusing on future employment. Starting in May 2020, Anna will start working as a full-time Software/Aerospace Engineer for L3Harris Technologies in Arlington, Texas.